Atmospheric Environment 45 (2011) 5903–5912

Contents lists available at ScienceDirect

Atmospheric Environment

journal homepage: www.elsevier.com/locate/atmosenv

Inverse modeling analysis of soil dust sources over East Asia

Bonyang Ku[a,b], Rokjin J. Park[a,*]

[a] School of Earth and Environmental Sciences, Seoul National University, Seoul 151-742, Republic of Korea

[b] National Institute of Meteorological Research, Seoul 156-720, Republic of Korea

ARTICLE INFO

Article history:
Received 29 March 2011
Received in revised form
18 June 2011
Accepted 21 June 2011

Keywords:
Inverse modeling
Soil dust
Dust emission
Particulate matter
Chemical transport model

ABSTRACT

Soil dust is the dominant aerosol by mass concentration in the troposphere and has considerable effects on air quality and climate. Parts of East Asia, including southern Mongolia, northern China, and the Taklamakan Desert, are important dust source regions. Accurate simulations of dust storm events are crucial for protecting human health and assessing the climatic impacts of dust events. However, even state-of-the-art aerosol models still contain large uncertainties in soil dust simulations, particularly for the dust emissions over East Asia. In this study, we attempted to reduce these uncertainties by using an inverse modeling technique to simulate dust emissions. We used the measured mass concentration of particles less than 10 μm in aerodynamic diameter (PM_{10}) in the surface air over East Asia, in combination with an inverse model, to understand the dust sources. The global three-dimensional GEOS-Chem chemical transport model (CTM) was used as a forward model. The inverse model analysis yielded a 76% decrease in dust emissions from the southern region of the Gobi Desert, relative to the a priori result. The a posteriori dust emissions from the Taklamakan Desert and deserts in eastern and Inner Mongolia were two to three fold higher than the a priori dust emissions. The simulation results with the a posteriori dust sources showed much better agreement with these observations, indicating that the inverse modeling technique can be useful for estimation of the optimized dust emissions from individually sourced regions.

1. Introduction

Soil dust aerosols are the largest contributor to aerosol mass concentrations in the troposphere (Forster et al., 2007) and influence global climate by affecting the radiation budget (Sokolik and Toon, 1996) and biogeochemical cycling (Jickells et al., 2005). In addition, soil dust aerosols play an important role in atmospheric chemistry by providing a surface area for heterogeneous reactions. The resulting poor air quality can lead to problems ranging from degraded visibility to respiratory illnesses (Kwon et al., 2002; Prospero, 1999).

Dust aerosols are naturally produced by wind erosion of the Earth's crust, a complicated process affected by numerous meteorological and surface conditions including surface wind speed, friction velocity, soil temperature, soil moisture, soil texture, land-use type, and snow and vegetation cover (Kurosaki and Mikami, 2004). Among the many dust source regions in arid and semi-arid areas, the Sahara Desert in North Africa is the most important, contributing 50–70% of annual global soil dust aerosol emissions (Tanaka and Chiba, 2006).

East Asia is also an important source region, accounting for 3–11% of global dust emissions (Tanaka and Chiba, 2006). More importantly, the dust source regions in East Asia are close to populated areas. East Asian dust storm outbreaks are common in spring over Mongolia and the Taklamakan and Gobi deserts and can result in substantial economic losses and environmental damage (Seinfeld et al., 2004). In favorable synoptic conditions, Asian dust aerosols can be transported across the Pacific, affecting the air quality in the western United States (Husar et al., 2001; Zhao et al., 2008).

Previous studies have applied three-dimensional (3-D) regional air quality models to simulate dust aerosols over East Asia (Gong et al., 2003; Park and In, 2003; Uno et al., 2003). A dust model inter-comparison (DMIP) study examined the current regional dust models applied to the Asian domain (Uno et al., 2006) and concluded that the dust aerosol transport patterns from the source regions were usually very similar, while the simulated dust concentrations in the surface air sometimes differed by over two orders of magnitude in the dust source regions. The simulation discrepancies are mainly attributable to uncertainties in the dust

* Corresponding author. Tel.: +82 2 880 6715; fax: +82 2 883 4972.
E-mail address: rjpark@snu.ac.kr (R.J. Park).

1352-2310/$ – see front matter
doi:10.1016/j.atmosenv.2011.06.078

emission simulations, which are typically parameterized by wind speed, soil water content, and vegetation cover (Marticorena and Bergametti, 1995; Tegen and Fung, 1994). Reducing these uncertainties and accurately quantifying dust emissions are critical for improving dust model capabilities.

In this study, we attempt to estimate the optimized dust sources in East Asia by applying an inverse modeling method, which minimizes the errors of a priori dust aerosol sources in the model with observational constraints to obtain optimized a posteriori sources. This approach allows for better understanding of the source strength changes and physical processes determining dust emissions over Asia. Previous studies using inverse modeling have focused on constraining anthropogenic emissions of carbon monoxide (Heald et al., 2004; Palmer et al., 2003), methyl chloride (Yoshida et al., 2006), ammonia (Gilliland et al., 2006), methane (Bergamaschi et al., 2005), carbon dioxide (Mueller et al., 2008), and black carbon (Hakami et al., 2005). The adjoint inversion modeling was applied to dust emissions (Yumimoto et al., 2008, 2007) using lidar observations but to our knowledge, this study is the first attempt to apply inverse modeling to dust emissions using surface layer measurements over East Asia.

Our approach was to use the observed particulate matter concentrations (PM_{10}, particles less than 10 μm in aerodynamic diameter) in the surface air, together with a 3-D global chemical transport model (GEOS-Chem) as a forward model for April 2001. Section 2 provides details regarding GEOS-Chem, an inverse model, and the observations used in the best estimation of dust sources. A model evaluation with a priori sources is presented in Section 3, and the results of the a posteriori sources of dust aerosols are described in Section 4. We discuss the simulation issues with the inverse modeling of dust emissions in Section 5. Our conclusions are summarized in Section 6.

2. Methods and data

Our objective in this study is to obtain optimized a posteriori dust emissions over East Asia. To achieve this, we applied inverse modeling analysis to measured PM_{10} mass concentrations in the surface air because dust aerosol observations are very scarce over East Asia. We focused on the April 2001 period, when severe dust storms occurred over East Asia. Observations were used to estimate the optimized dust emissions; the magnitude and variability of PM_{10} mass concentrations are primarily explained by those of the dust aerosol concentrations during dust storm outbreaks. The results yielded the best estimates of the dust sources in East Asia.

2.1. Forward model

We used a global 3-D chemical transport model (GEOS-Chem) to conduct aerosol simulations, including of dust aerosol over East Asia (Fairlie et al., 2007; Park et al., 2004). The model (v.8.1.1, http://acmg.seas.harvard.edu/geos/index.html) has a horizontal resolution of 2° latitude × 2.5° longitude with 30 vertical levels from the surface to 0.01 hPa and is driven by GEOS-3 assimilated meteorological data from the Goddard Earth Observing System (GEOS) of the NASA Global Modeling and Assimilation Office (GMAO). The GEOS-Chem was applied for an inter-comparison study of CTM simulations of CO during the Transport and Chemical Evolution over the Pacific mission period and showed no bias in GEOS-Chem transport driven by GEOS-3 assimilated meteorological data (Kiley et al., 2003).

Aerosol simulations in GEOS-Chem have been described in detail elsewhere (Fairlie et al., 2007; Park et al., 2004, 2006). Here, we briefly discuss our dust simulation model. For soil dust mobilization, we used the dust entrainment and deposition (DEAD) scheme of Zender et al. (2003a,b) that treats the vertical dust flux as proportional to the horizontal saltation dust flux based on the theory of White (1979). In the model the sandblasting is expressed simply as a function of the mass fraction of clay particles in the parent soil and the clay fraction in soil is assumed to be constant that might possess nontrivial uncertainty. In addition, the threshold friction velocity, at which soil particles begin to be mobilized, is assigned to be a fixed value for smooth dry surface. Although the impacts of soil moisture and vegetation cover on the threshold friction velocity are taken into account with a correction factor we acknowledge possible errors caused by the present approach adding some uncertainties to dust mobilization in the model. Size-segregated dust aerosols were computed using the tri-modal lognormal probability density function that was arranged into four size bins (radii 0.1–1.0, 1.0–1.8, 1.8–3.0, and 3.0–6.0 μm). The dry deposition of dust aerosol is represented with a deposition velocity that is defined by the gravitational settling and turbulent transfer of particles to the surface (Seinfeld and Pandis, 1998; Zhang et al., 2001). The wet deposition process for dust aerosol includes scavenging in convective updrafts and rainout and washout from large-scale precipitation and convective anvils (Liu et al., 2001).

The major source regions of soil dust aerosols over Asia include the deserts in Mongolia and western and northern China, including the Taklamakan and Gobi deserts. Other arid regions in northeastern China and Inner Mongolia have become important soil dust sources as desertification and deforestation progress along with industrialization and climate changes (Chin et al., 2003; Lim and Chun, 2006). To quantify the dust source contributions from different source regions, we conducted tagged dust aerosol simulations, which carry separate dust aerosol tracers from individual source regions (Zhang et al., 2003b). The model computes the dust concentrations, which are calculated with geographically separated dust emissions from 11 dust source regions as shown in Fig. 1. These include the deserts and sands in Kazakhstan (S1), the Mongolian Plateau (S2), the Taklamakan Desert (S3), the Tsaidam basin and Kumutage Desert (S4), the Badan Jaran, Tengger, and Ulan Buh deserts (S5), the Mu Us and Hobq deserts (S6), the Onqin Dega sandy land (S7), the Horqin sandy land (S8), historical deposition areas (S9 and S10), and the rest of the world (RoW). Forward model simulations were conducted for the tagged dust aerosols and non-dust aerosols from January to May 2001, with our analysis focusing primarily on 1 April–10 May 2001, a period in which intense dust storms affected East Asia.

2.2. Inverse model

Our inverse model defines the strength of the dust emissions from the individual source regions shown in Fig. 1 as a state vector that was optimized using observations based on the Bayesian least-squares method. Dust aerosol concentrations are determined by emission, dry and wet deposition, and transport as described in the previous section. Changes in dust aerosol concentrations to these processes are all first-order dependent. In particular, dust aerosol concentrations vary linearly depending upon dust emissions. As shown in Equation (1), the observation vector $\mathbf{y}$ represents the assembled PM_{10} measurements in the surface air that can be related to the state vector $\mathbf{x}$ of the dust aerosol emissions:

$$\mathbf{y} = \mathbf{K}\mathbf{x} + \varepsilon \tag{1}$$

The Jacobian matrix $\mathbf{K}$ indicates the forward model (as described in the previous section) and does not depend on the state vector under our linear assumption that is to relate the sources to the concentrations in a forward sense. Since PM_{10} mass concentrations may include fractions of non-dust aerosols even during severe dust

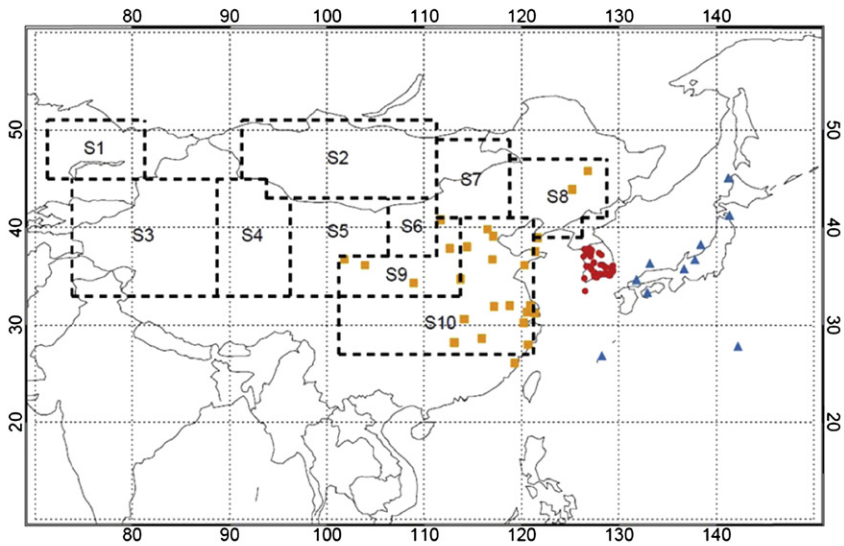

Fig. 1. Dust source regions are divided into 10 source areas (S1–S10) and the rest of the world (RoW). Locations of PM_{10} observation sites in China ($n = 26$), Korea ($n = 110$), and Japan ($n = 10$) are denoted with yellow squares, red dots, and blue triangles, respectively. (For interpretation of the references to color in this figure legend, the reader is referred to the web version of this article.)

storm periods, we added a state vector that represents the sum of non-dust aerosol emissions including sulfate, nitrate, ammonium, black carbon, organic carbon, and sea salt aerosols over East Asia. The error vector $\boldsymbol{\varepsilon}$ includes contributions from the measurement accuracy, subgrid variability of the observations, and errors in the forward model. The characteristics of these errors are described by the observational error covariance ($\mathbf{S}_\varepsilon$) below.

The optimized a posteriori state vector ($\hat{\mathbf{x}}$) (Rodgers, 2000) is given as follows:

$$\hat{\mathbf{x}} = \mathbf{x_a} + \left(\mathbf{K}^{\mathrm{T}}\mathbf{S}_\varepsilon^{-1}\mathbf{K} + \mathbf{S}_\mathbf{a}^{-1}\right)^{-1}\mathbf{K}^{\mathrm{T}}\mathbf{S}_\varepsilon^{-1}(\mathbf{y} - \mathbf{K}\mathbf{x_a}) \quad (2)$$

where $\mathbf{x_a}$ is the a priori state vector and $\mathbf{S_a}$ is the error covariance matrix for the a priori state vector ($\mathbf{x_a}$). The superscript T represents the transpose operator of a matrix. The a posteriori error covariance matrix ($\hat{\mathbf{S}}$) is computed as follows:

$$\hat{\mathbf{S}} = \left(\mathbf{K}^{\mathrm{T}}\mathbf{S}_\varepsilon^{-1}\mathbf{K} + \mathbf{S}_\mathbf{a}^{-1}\right)^{-1} \quad (3)$$

The error covariance ($\mathbf{S_a}$) of the a priori state vector ($\mathbf{x_a}$) is assigned an uncertainty of 200% for individual dust source estimates, based on recent global model estimates of dust emissions, which differ by more than a factor of two (Miller et al., 2004; Werner et al., 2002). For dust emissions from the rest of the world (RoW) and non-dust aerosol emissions, the error of the a priori state vector is arbitrarily assigned an uncertainty of 10% for each source. This value is relatively lower than the former uncertainty value because our main focus is the best estimation of dust sources over East Asia.

The observational error covariance ($\mathbf{S}_\varepsilon$) can be decomposed into a sum of error covariance matrices describing the instrument error, the representation error, and the forward model error. The forward model error is assumed to be 93% based on the relative difference between the PM_{10} observations and the colocated model PM_{10} concentrations with a priori sources, as represented by $(\mathbf{K}\mathbf{x_a} - \mathbf{y})/\mathbf{y}$. We assumed that the mean bias is due to errors in the a priori sources and that the variance about this mean value represents uncertainty due to the model (Palmer et al., 2003). The representation error is 83%, which is calculated by the standard deviation of the observed PM_{10} concentration from its mean value. The instrumental error of the PM_{10} mass concentrations is assigned an uncertainty of 10%. The sensitivity of the a posteriori solution to the associated error estimations and the data selection are assessed in Section 5.

2.3. Data

We used daily observations of PM_{10} mass concentrations in the surface air over East Asia. The observed PM_{10} concentrations are measured with automatic instruments using the β-ray absorption method and the Tapered Element Oscillating Microbalance method in China as well as Korea and Japan. The used PM_{10} concentrations are quantitative measures for uniformly monitoring mass concentrations of particles less than 10 μm in aerodynamic diameter in the surface air. These instruments errors for particulate matter measures are 2%–9% which are relatively small to the total temporal variability (Goldman et al., 2009). The data were obtained from the Chinese Ministry of Environmental Protection (MEP, formerly SEPA, http://datacenter.mep.gov.cn), the Korean Ministry of Environment (MOE, http://www.airkorea.or.kr), and the Acid Deposition Monitoring Network (EANET, http://www.eanet.cc) in Japan.

The observed PM_{10} concentrations over China are derived from the ambient air pollution index (API), which is a semi-quantitative measure, designed to uniformly report the air quality in China. At each observational site, the concentrations of PM_{10}, SO_2, and NO_2 are automatically measured and a corresponding API value is reported as a dimensionless number from 0 to 500 for the highest pollutant concentration on a given day. The pollutant type on a given day is also inferred, except for "clean" days when the API value is below 50 (i.e., the concentrations of NO_2, SO_2, and PM_{10} are below 80, 50, and 50 μg m^{-3}, respectively). Here we considered only the PM_{10}-polluted days and clean days. Details on the API data and calculation of PM_{10} concentrations from APIs can be found in previous studies (Choi et al., 2009; Gong et al., 2007; Zhang et al., 2003a). PM_{10} concentrations converted from APIs in China were associated with dust storm propagation (Chu et al., 2008). The available 26 Chinese observation sites are located in central-eastern China (east of 100°E) and are affected by dust outbreaks in spring.

In Korea, PM_{10} concentrations are routinely observed across the country. The observed daily PM_{10} mass concentrations were available at 110 sites in 42 cities in Korea. The majority of sites were in urban areas. The Korean government releases quality-assured (QA) and quality-controlled (QC) data in which abnormal values are filtered out through the data screening process.

The EANET project was initiated to improve our understanding of the acid deposition problem in East Asia. Since January 2001, regular measurements of aerosol species concentrations have been conducted, including measurements of gaseous pollutants, soluble aerosols, and PM_{10}. We used the daily PM_{10} concentrations from 10 EANET sites in Japan. These sites are mainly located on islands and in rural and mountainous regions to avoid the direct influence of a local source. All the observed PM_{10} concentrations discussed were averaged to the corresponding $2^\circ \times 2.5^\circ$ horizontal grids to estimate dust emissions and compare with the model.

To evaluate the optimized dust sources independently, we used the aerosol index (AI) data of the Earth Probe Total Ozone Mapping Spectrometer (TOMS) and the aerosol optical depth (AOD) data from the Multi-angle Imaging Spectrometer (MISR) on-board the Earth Observing System (EOS) Terra satellite. TOMS AI is an excellent indicator of the presence of UV-absorbing aerosols, such as mineral dust and black carbon (Herman et al., 1997; Torres et al., 1998). Although TOMS AI is more sensitive to UV-absorbing aerosols at altitudes above 2 km and is distorted by the presence of clouds, it detects considerable dust activity (Prospero et al., 2002). MISR/Terra (Diner et al., 2001) provides near-global coverage of the AOD data in four narrow spectral bands centered at 446, 558, 672, and 866 nm. MISR can retrieve aerosol properties over a variety of terrains, including reflective surfaces such as deserts (Martonchik et al., 2004). We used the level-3 AOD products at 558 nm wavelength, gridded at a horizontal resolution of $0.5^\circ \times 0.5^\circ$ from MISR.

3. Model evaluation with a priori sources

In spring 2001, intense Asian dust storms occurred on several occasions (Darmenova et al., 2005; Gong et al., 2003). Among these, a particularly strong dust storm occurred over the Taklamakan Desert and deserts in China and Mongolia on 6 April 2001 (Liu et al., 2003). This dust storm moved eastward to northeastern China, resulting in widespread poor visibility in northern China. The dust reached the Korean peninsula on 8 April and Japan on 9 April (Gong et al., 2003; Liu et al., 2003). This East Asian dust storm was the most severe event on record and significantly affected surface PM concentrations as far as the United States (Jaffe et al., 2003; Zhao et al., 2008). The other major dust storm in April 2001 began in the Taklamakan and Gobi deserts on 29 April (Gong et al., 2003). In this case, dust aerosols were transported directly eastward by strong meridional flow promoted by a deep trough formed west of Japan. This dust storm affected downwind regions such as Korea and Japan and the west coast of North America to a lesser extent (Gong et al., 2003).

We focused on these well-documented dust events to evaluate the model output. The left panels in Figs. 2–4 show comparisons between the observed and simulated PM_{10} mass concentrations with a priori sources at sites in China, Korea, and Japan. The high modeled PM_{10} concentrations are mainly the result of dust aerosols from the southern region of the Gobi Desert (S5; blue colored) and deserts in northeastern China (S8; orange colored) and Mongolia (S2; red colored). During the dust events, the modeled concentrations are generally higher than the observations near the source regions of China. Dust aerosol from the southern Gobi Desert is

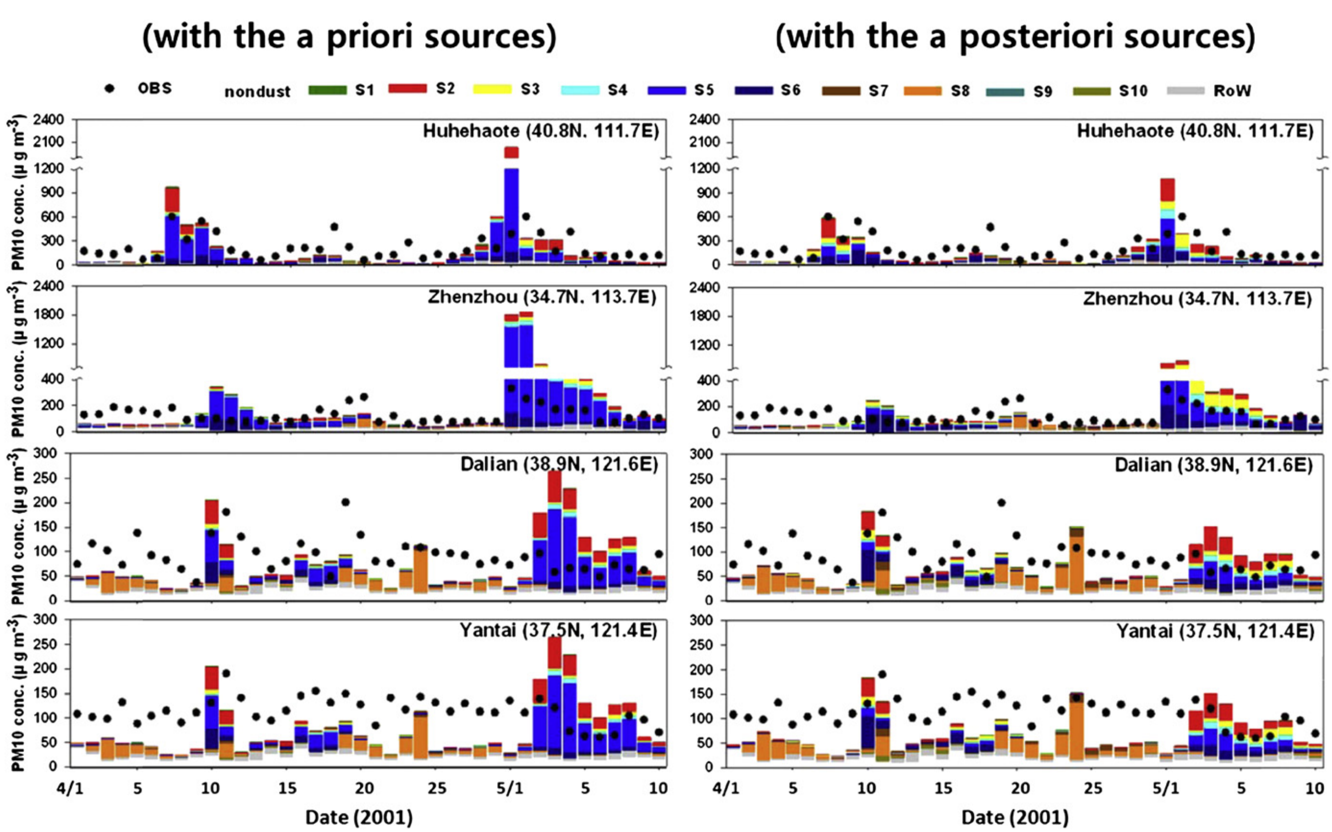

Fig. 2. Observed daily PM_{10} concentrations versus modeled PM_{10} concentrations with the a priori emissions (left) and the a posteriori emissions (right) at Huhehaote, Zhenzhou, Dalian, and Yantai in China. Black dots show observations and colored bars show simulated concentrations. Different colors indicate the individual contributions of soil dust aerosols from each source region; non-dust aerosols are shown in white. (For interpretation of the references to color in this figure legend, the reader is referred to the web version of this article.)

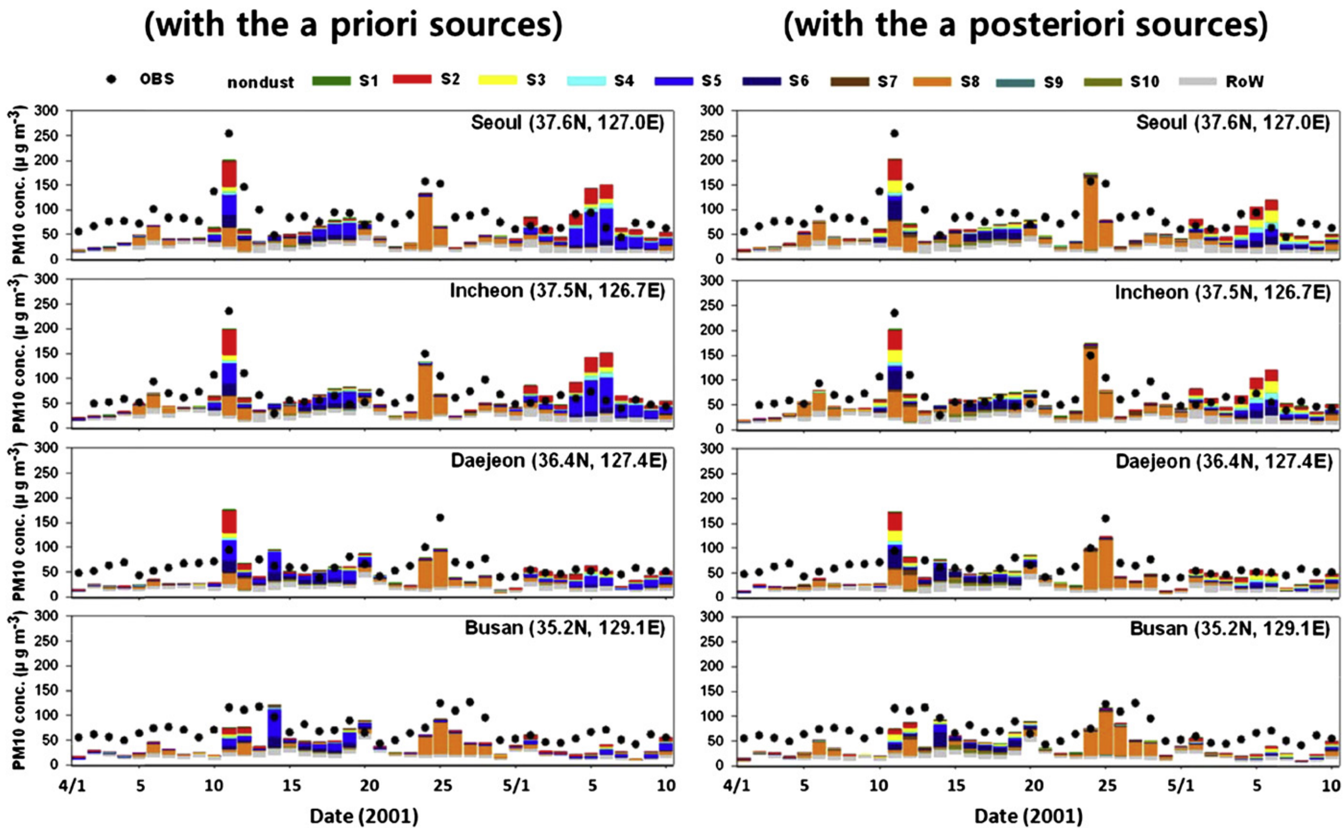

Fig. 3. Same as in Fig. 2 but at Seoul, Incheon, Daejeon, and Busan in Korea. (For interpretation of the references to color in this figure legend, the reader is referred to the web version of this article.)

a major contributor to the high PM_{10} concentrations in the model. From the end of April to the beginning of May, the model shows remarkably higher PM_{10} concentrations compared to the observations over China, particularly at Huhehaote and Zhenzhou that are located close to the dust source regions. These elevated PM_{10} concentrations in the model mainly result from the high contribution from the southern region of the Gobi Desert.

Korea and Japan were also affected by the two dust outbreaks in April. The first event affected Korea from 9 to 14 April, and hourly averaged PM_{10} concentrations in Seoul exceeded 800 $\mu g\ m^{-3}$ on 11 April. This dust primarily originated from the Gobi Desert and affected the middle of the Korean peninsula and southwestern Japan most significantly. Busan, in southern Korea, appeared less affected by this dust outbreak than Seoul and Incheon which are located relatively north. The model reproduced the observed PM_{10} concentrations in Korea relatively well. However, at sites in Japan, the simulated PM_{10} concentrations exceeded observed concentrations during this period because of the high dust aerosol concentrations from the Gobi Desert in the model. Dissimilar transport pathways of the dust aerosols resulted in different source contributions to the PM_{10} concentrations in downwind regions. The second dust event from 24 to 26 April reached a peak PM_{10} concentration of 920 $\mu g\ m^{-3}$ in Korea on 24 April. This dust was primarily from Inner Mongolia and Manchuria, which are located closer than other source regions to Korea. The dust aerosols from these sources more directly affected Korea.

In contrast, model values were generally lower than observations during non-dust storm periods, even at sites close to the source regions. We attribute this low bias to a lack of fugitive dust emissions in the model. Fugitive dust from unpaved roads, agricultural soil, construction, and disturbed surfaces in local regions substantially contributes to the fraction of PM_{10} mass concentrations. Huang et al. (2010) reported that the main local contributions of PM_{10} in Beijing were stationary emissions, road dust emissions, construction site dust emissions, and fugitive industrial emissions that accounted for 60% of the total emission sources. Moreover, Jang et al. (2008) estimated that fugitive dust emissions accounted for three quarters of the total PM_{10} emissions in the capital region of Korea.

4. A posteriori sources of dust aerosols

Here, we present our optimized dust sources over East Asia from inverse modeling analysis and evaluate them by comparison with the observations. The a priori dust sources discussed above yielded 38.2 Tg over Asia (10–60°N, 70–150°E) in April 2001. The dominant source region was the southern area of the Gobi Desert (S5), contributing ~40% of the total dust emission, followed by Mongolia (S2) and the Taklamakan Desert (S3), which accounted for 21% and 14%, respectively. Fig. 5 shows the modeled dust emissions and concentrations with the a priori and a posteriori sources over East Asia. The simulated total dust emission with the a posteriori source was 35.4 Tg, slightly lower than the a priori value. Although there was only a slight change in the magnitude of total emissions between the a priori and a posteriori results, the spatial distribution of dust emissions was significantly altered.

Regions in which dust emissions changed significantly with the a posteriori sources were the southern regions of the Gobi Desert (S5), the Taklamakan Desert (S3), eastern Mongolia and Inner Mongolia (S7), and Manchuria (S8). Over the Gobi Desert in China (S5), the a posteriori emission decreased by 76% relative to the a priori emission. Over the Taklamakan Desert (S3) and eastern and

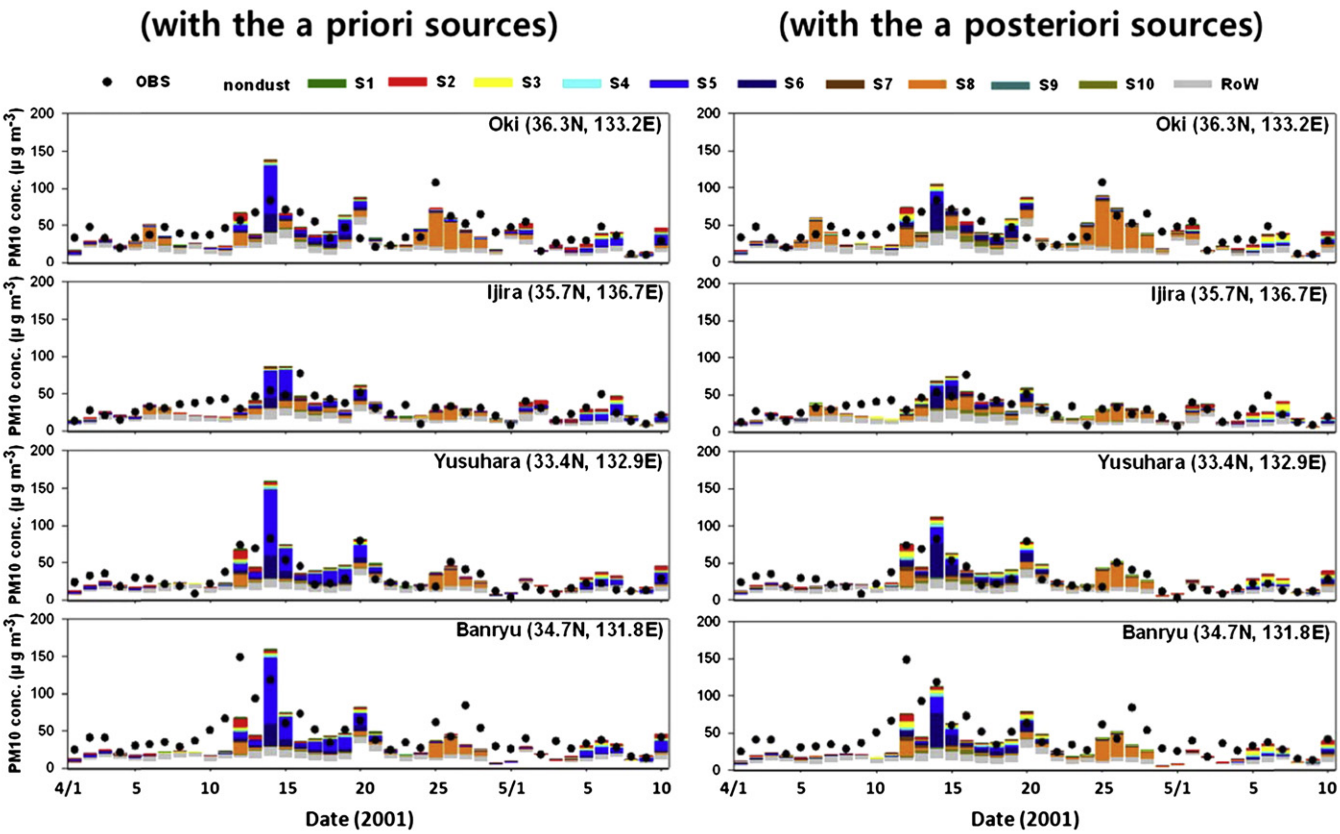

Fig. 4. Same as in Fig. 2 but at Oki, Ijira, Yusuhara, and Banryu in Japan. (For interpretation of the references to color in this figure legend, the reader is referred to the web version of this article.)

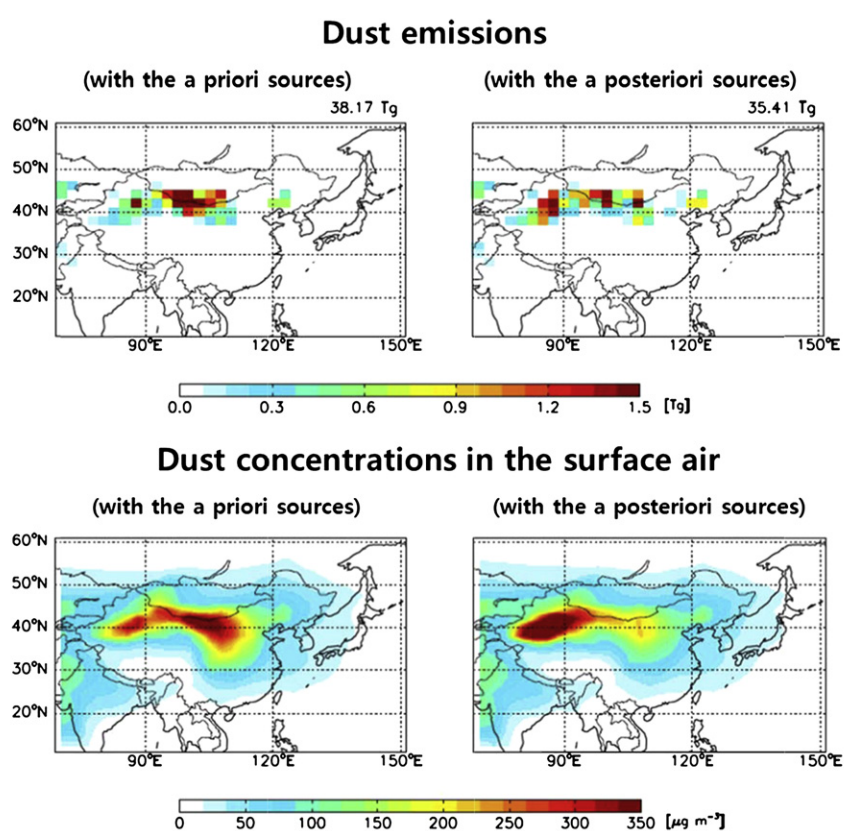

Fig. 5. Simulated dust emissions (upper) and surface air dust concentrations (lower) with the a priori (left) and a posteriori dust sources (right).

Inner Mongolia (S7), the a posteriori sources increased two to three fold compared to the a priori sources. The a posteriori source in Manchuria (S8) also increased by 36% compared to the a priori source. The Manchuria source region is close to the Korean peninsula and the resulting change improved the simulations in Korea. The a posteriori sources over historical deposition areas (S9 and S10) increased by 26% and a factor of 3, respectively. However, the effects of these changes on PM_{10} concentrations are trivial, as these areas are minor source regions accounting for less than 1% of the dust emissions over East Asia. Changes in the individual source regions are summarized in Table 1.

Figs. 2–4 also compare the observed versus simulated PM_{10} concentrations using the a posteriori sources in China, Korea, and Japan. The large bias with the a priori sources during the dust events (7–14 April, 29 April–5 May) is significantly reduced and the model shows better agreement with the observations. During 1 April–10 May, the mean bias decreased from 82% to 65% in China. For downwind regions, the mean bias decreased from 41% to 38% in Korea and from 52% to 49% in Japan. This improvement is largely due to decreased dust emissions from the southern Gobi Desert and increased emissions from northeastern China.

To additionally verify our results from the inverse modeling analysis, we compared the spatial distributions of the monthly mean TOMS AI with simulated column concentrations of dust and black carbon aerosols in April 2001 (Fig. 6). The model results were sampled at 00–07 UTC for the satellite overpass time when the observations were available in East Asia. Horizontal resolutions of TOMS AI and model simulations are $1.0^\circ \times 1.25^\circ$ and $2.0^\circ \times 2.5^\circ$, respectively. The TOMS AI indicates the magnitude of UV-absorbing aerosols, such as mineral dust and black carbon. The highest TOMS AI values were found in the Taklamakan Desert; values were also generally large in the Gobi Desert. The high values likely reflect the presence of absorbing dust aerosols because no apparent sources of black carbon aerosols are present in these arid areas. The simulated dust column concentrations with the a posteriori sources reproduced the spatial distributions of TOMS AI very well, relative to the a priori sources.

We also compared simulated and observed monthly mean AOD values from satellite measurements. We calculated AOD during 00–07 UTC for the satellite overpass time in East Asia using the Mie algorithm (Wiscombe, 1980) and physical parameters of all aerosols including the effective dry diameters and the refractive indices from Chin et al. (2002). Fig. 7 shows AOD from MISR observations (Diner et al., 2001) and the simulated values with the a priori and a posteriori sources in April 2001. The horizontal resolution of MISR data is $0.5^\circ \times 0.5^\circ$ and white areas indicate missing data. Scales of color bars are different for observations and simulations. MISR AODs were high in the Taklamakan Desert, eastern China, and the northwestern Pacific Ocean. The AODs simulated with the a posteriori sources showed a similar spatial pattern and much better agreement with the observations relative to the a priori simulations.

The use of a posteriori sources enabled us to better quantify the spatial and temporal distributions of dust aerosol concentrations and

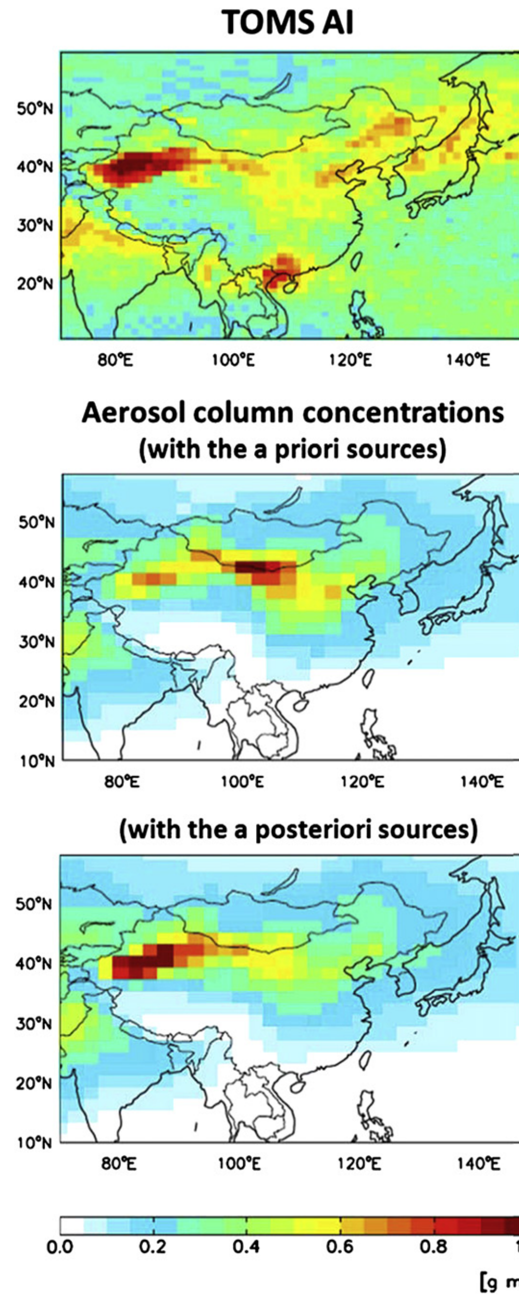

Fig. 6. Aerosol Index (AI) from the Total Ozone Mapping Spectrometry (TOMS) versus modeled column concentrations of black carbon and dust aerosols with the a priori and a posteriori dust sources in April 2001. The horizontal resolutions of TOMS AI and model simulations are $1.0^\circ \times 1.25^\circ$ and $2.0^\circ \times 2.5^\circ$, respectively.

Table 1
Inverse modeling analysis of dust sources over East Asia in the domain 10–60°N, 70–150°E for April 2001.

	Regions											
	S1	S2	S3	S4	S5	S6	S7	S8	S9	S10	RoW	Total
A priori sources (Tg mon^{-1})												
Emissions (%)	0.33 (0.9)	8.03 (21.0)	5.51 (14.4)	3.14 (8.2)	15.39 (40.3)	2.60 (6.8)	0.11 (0.3)	1.63 (4.3)	0.02 (0.1)	0.07 (0.2)	1.34 (3.5)	38.17 (100)
A posteriori sources (Tg mon^{-1})												
Emissions (%)	0.35 (1.0)	6.30 (17.8)	12.94 (36.5)	3.92 (11.1)	3.69 (10.4)	4.00 (11.3)	0.34 (1.0)	2.21 (6.2)	0.03 (0.1)	0.18 (0.5)	1.44 (4.1)	35.42 (100)
Ratios (*a posteriori/a priori*)												
Ratios	1.1	0.8	2.3	1.2	0.2	1.5	3.0	1.4	1.3	2.6	1.1	

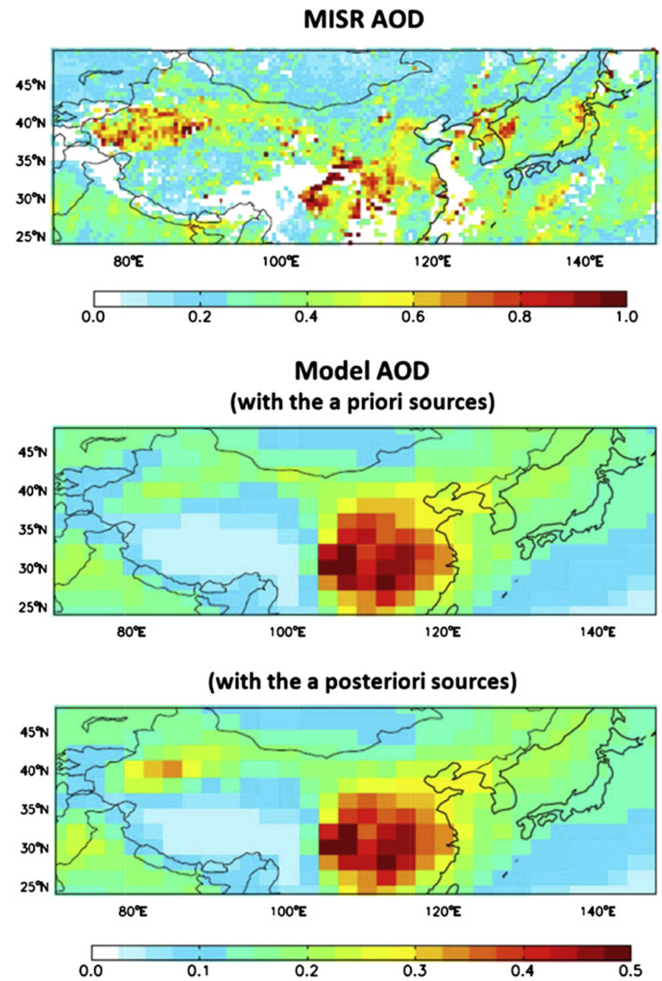

Fig. 7. Monthly mean aerosol optical depths (AODs) from the Multi-angle Imaging Spectrometer (MISR) versus model values from the a priori and a posteriori sources in April 2001. The horizontal resolution of MISR data is 0.5° × 0.5° and white areas indicate missing data. Note the difference in color scales. (For interpretation of the references to color in this figure legend, the reader is referred to the web version of this article.)

their contributions to air quality over East Asia. Our inverse modeling analysis also identified weaknesses in dust models reported in previous studies. For example, Tanaka and Chiba (2006) demonstrated that a model with coarse spatial resolution underestimated the dust emissions from the Taklamakan Desert because of insufficient representation of local wind. One of the challenges in dust modeling is to realistically represent subgrid-scale wind erosion processes at coarse model resolutions typically of more than 100 km. Lim and Chun (2006) reported that blowing sand events were becoming more frequent in Inner Mongolia as Asian dust source regions extended eastward from the Gobi, Tengger, and Ordos deserts to Inner Mongolia and northeast China, driven by eastward expanding desertification. In addition, eastern Mongolia, Inner Mongolia, and Manchuria (China) have been suggested as major areas of desertification in recent decades (Chin et al., 2003). These observations are remarkably consistent with the changes in the inverse modeling results from a priori to a posteriori sources.

5. Issues with the inverse modeling analysis of dust emissions

Our inverse modeling indicated that dust emissions in the southern regions of the Gobi Desert should substantially decrease, while increases were expected over the Taklamakan Desert and northeastern China. However, our results have some limitations. First, the strength and frequency of dust outbreaks display strong inter-annual variability, meaning that the best estimates of dust sources based on a single year observation may have considerable uncertainties. To overcome this issue, the physical processes responsible for dust source changes and the variations in these processes must be clarified by analysis of long-term observations.

In our analysis, we used measured PM_{10} concentrations because no direct dust observations were available over East Asia. These PM_{10} concentrations may not completely represent the dust aerosol concentrations. In addition, the PM_{10} concentrations in China retrieved from the API data have a cap of 600 μg m^{-3} that comprises about 2% of the data. These capped measurements may cause a low bias for tremendously strong dust storms. The use of direct dust observations both in the surface air and aloft would allow for better quantification of dust emissions and the 3-D distribution of dust aerosol concentrations over Asia.

Furthermore, we used uncertainty values of 200% for the individual dust sources over East Asia, 10% for the rest of global dust sources and non-dust aerosol emissions, and also 10% for the instrumental error of the PM_{10} mass concentrations. These uncertainties were arbitrarily assigned. To examine the sensitivity of the a posteriori sources to the assumed uncertainty values, we performed several analyses using different data sets and errors. Fig. 8 shows a comparison between the a priori dust sources and the a posteriori dust sources from our sensitivity analyses. Cases 1–2 are

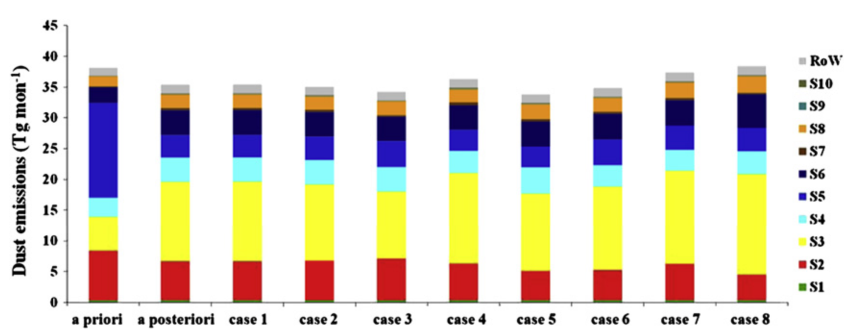

Fig. 8. Estimates of dust emissions for each source region from the inverse modeling analysis. Values with a priori source are the forward model results and a posteriori is our best estimates. Each case shows the sensitivity results using different errors and data selections. Cases 1 and 2 show results with 1% and 50% instrumental errors, respectively, and cases 3 and 4 are derived with 150% and 250% errors, respectively, for dust sources using all PM_{10} observations from China, Korea, and Japan. Case 5 is the result from assigning different transport errors of 100%, 30%, and 70% for China, Korea, and Japan. Cases 6–8 are obtained with 200% dust source errors and 93% transport error and with different data selections. The data for case 6 include the PM_{10} observations from China alone. In cases 7 and 8, the PM_{10} observations above 50 μg m^{-3} and 100 μg m^{-3}, respectively, from China, Korea, and Japan were used.

results from the same condition described above, except for 1% and 50% instrumental errors, respectively. These results are consistent with the previous a posteriori sources. Cases 3–4 have 150% and 250% errors, respectively, for dust sources using all the PM_{10} observations from China, Korea, and Japan. Case 5 is result from assigning different transport errors of 100%, 30%, and 70% for China, Korea, and Japan that are estimated by calculating the difference between the observations and models in each country. Cases 6–8 have 200% dust sources error and 93% transport error for different data selections. The data for case 6 include the PM_{10} observations from China alone. In cases 7 and 8, the PM_{10} observations above 50 and 100 $\mu g\ m^{-3}$ from China, Korea, and Japan were used, respectively. Although the a posteriori emissions for each case differ slightly, the contributions of each source region in the a posteriori dust emissions show a consistent change when compared with the a priori sources, indicating the robustness in our inverse model analysis.

6. Conclusions

We applied an inverse model to obtain optimized a posteriori dust emissions in April 2001. The PM_{10} mass concentrations in the surface air were used as direct dust aerosol observations that were very scarce over East Asia. This study presents a first attempt to apply inverse modeling to soil dust aerosol emissions from different geographical source regions over East Asia, using PM_{10} observations in the surface air. The GEOS-Chem global 3-D chemical transport model was used as a forward model to simulate the PM_{10} concentrations including non-dust in addition to dust aerosols.

First, the forward model was evaluated by comparing simulated PM_{10} mass concentrations to observations in China, Korea, and Japan, focusing on the dust outbreak events in April 2001. During these dust events, the model was generally higher than the observations near the dust source regions in China, mainly due to the high dust emissions from the Gobi Desert.

Our inverse modeling analysis indicated that the a priori dust emissions from the southern part of the Gobi Desert (S5) were too high, while those from the Taklamakan Desert (S3), eastern Mongolia, and Inner Mongolia (S7) were too low. The resulting a posteriori source in the southern Gobi Desert was 3.7 Tg mon^{-1}, representing a decrease of 76% from the a priori source. Meanwhile, over the Taklamakan Desert (S3), the a posteriori emissions (12.9 Tg mon^{-1}) were two times larger than the a priori emissions and the a posteriori sources in Manchuria (S8) increased by 36% and amounted to 2.2 Tg mon^{-1}. The Manchuria source region is close to the Korean peninsula and the resulting change improved the simulation when compared to the observations in Korea. Over eastern and Inner Mongolia (S7), the a posteriori sources also increased by a factor of three, but the absolute increase was relatively marginal. Overall, the total simulated dust emissions over East Asia (10–60°N, 70–150°E) decreased only slightly ($\sim$7%) from the a priori to the a posteriori sources in April 2001, but improved the spatial pattern of the simulated PM_{10} concentrations, resulting in a much better agreement with the observations. This study shows that the inverse modeling technique can be used to estimate the optimized dust emissions from individual source regions, allowing for improved quantification of the spatial and temporal distributions of dust aerosols and better understanding of air quality and climate change in East Asia.

Acknowledgments

This study was funded by the Korea Meteorological Administration Research and Development Program under Grant CATER 2007–3205.

References

Bergamaschi, P., Krol, M., Dentener, F., Vermeulen, A., Meinhardt, F., Graul, R., Ramonet, M., Peters, W., Dlugokencky, E.J., 2005. Inverse modelling of national and European CH_4 emissions using the atmospheric zoom model TM5. Atmospheric Chemistry and Physics 5, 2431–2460.

Chin, M., Ginoux, P., Kinne, S., Torres, O., Holben, B., Duncan, B., Martin, R., Logan, J., Higurashi, A., Nakajima, T., 2002. Tropospheric aerosol optical thickness from the GOCART model and comparisons with satellite and Sun photometer measurements. Journal of the Atmospheric Sciences 59, 461–483.

Chin, M., Ginoux, P., Lucchesi, R., Huebert, B., Weber, R., Anderson, T., Masonis, S., Blomquist, B., Bandy, A., Thornton, D., 2003. A global aerosol model forecast for the ACE-Asia field experiment. Journal of Geophysical Research 108, 8654.

Choi, Y., Park, R.J., Ho, C., 2009. Estimates of ground-level aerosol mass concentrations using a chemical transport model with Moderate Resolution Imaging Spectroradiometer (MODIS) aerosol observations over East Asia. Journal of Geophysical Research 114, D04204.

Chu, P.C., Chen, Y., Lu, S., Li, Z., Lu, Y., 2008. Particulate air pollution in Lanzhou China. Environment International 34, 698–713.

Darmenova, K., Sokolik, I.N., Darmenov, A., 2005. Characterization of east Asian dust outbreaks in the spring of 2001 using ground-based and satellite data. Journal of Geophysical Research 110, D02204.

Diner, D.J., Abdou, W.A., Bruegge, C.J., Conel, J.E., Crean, K.A., Gaitley, B.J., Helmlinger, M.C., Kahn, R.A., Martonchik, J.V., Pilorz, S.H., Holben, B.N., 2001. MISR aerosol optical depth retrievals over southern Africa during the SAFARI-2000 dry season campaign. Geophysical Research Letters 28, 3127–3130.

Fairlie, T.D., Jacob, D.J., Park, R.J., 2007. The impact of transpacific transport of mineral dust in the United States. Atmospheric Environment 41, 1251–1266.

Forster, P., Ramaswamy, V., Artaxo, P., Berntsen, T., Betts, R., Fahey, D.W., Haywood, J., Lean, J., Lowe, D.C., Myhre, G., Nganga, J., Prinn, R., Raga, G., Schulz, M., Dorland, R.V., 2007. Changes in atmospheric constituents and in radiative forcing. Climate change 2007: the physical science basis. In: Solomon, S., Qin, D., Manning, M., Chen, Z., Marquis, M., Averyt, K.B., Tignor, M., Miller, H.L. (Eds.), Contribution of Working Group I to the Fourth Assessment Report of the Intergovernmental Panel on Climate Change. Cambridge University Press, Cambridge, United Kingdom and New York, NY, USA.

Gilliland, A.B., Wyat Appel, K., Pinder, R.W., Dennis, R.L., 2006. Seasonal NH_3 emissions for the continental united states: inverse model estimation and evaluation. Atmospheric Environment 40, 4986–4998.

Goldman, G., Mulholland, J., Strickland, M., Tolbert, P., 2009. Assessment of ambient air pollutant measurement error associated with instrument precision and spatial heterogeneity. Epidemiology 20, S80.

Gong, D.-Y., Ho, C.-H., Chen, D., Qian, Y., Choi, Y.-S., Kim, J., 2007. Weekly cycle of aerosol-meteorology interaction over China. Journal of Geophysical Research 112, D22202.

Gong, S.L., Zhang, X.Y., Zhao, T.L., McKendry, I.G., Jaffe, D.A., Lu, N.M., 2003. Characterization of soil dust aerosol in China and its transport and distribution during 2001 ACE-Asia: 2. Model simulation and validation. Journal of Geophysical Research 108, 4262.

Hakami, A., Henze, D.K., Seinfeld, J.H., Chai, T., Tang, Y., Carmichael, G.R., Sandu, A., 2005. Adjoint inverse modeling of black carbon during the Asian Pacific regional aerosol characterization experiment. Journal of Geophysical Research 110, D14301.

Heald, C.L., Jacob, D.J., Jones, D.B.A., Palmer, P.I., Logan, J.A., Streets, D.G., Sachse, G.W., Gille, J.C., Hoffman, R.N., Nehrkorn, T., 2004. Comparative inverse analysis of satellite (MOPITT) and aircraft (TRACE-P) observations to estimate Asian sources of carbon monoxide. Journal of Geophysical Research 109, D23306.

Herman, J.R., Bhartia, P.K., Torres, O., Hsu, C., Seftor, C., Celarier, E., 1997. Global distribution of UV-absorbing aerosols from Nimbus 7/TOMS data. Journal of Geophysical Research 102, 16911–16922.

Huang, Q., Cheng, S.Y., Li, Y.P., Li, J.B., Chen, D.S., Wang, H.Y., 2010. An integrated MM5-CAMx modeling approach for assessing PM10 contribution from different sources in Beijing, China. Journal of Environmental Informatics 15, 47–61.

Husar, R.B., Tratt, D.M., Schichtel, B.A., Falke, S.R., Li, F., Jaffe, D., Gassó, S., Gill, T., Laulainen, N.S., Lu, F., Reheis, M.C., Chun, Y., Westphal, D., Holben, B.N., Gueymard, C., McKendry, I., Kuring, N., Feldman, G.C., McClain, C., Frouin, R.J., Merrill, J., DuBois, D., Vignola, F., Murayama, T., Nickovic, S., Wilson, W.E., Sassen, K., Sugimoto, N., Malm, W.C., 2001. Asian dust events of April 1998. Journal of Geophysical Research 106, 18317–18330.

Jaffe, D., Price, H., Parrish, D., Goldstein, A., Harris, J., 2003. Increasing background ozone during spring on the west coast of North America. Geophysical Research Letters 30, 1613.

Jang, Y., Kim, J., Kim, P., Shin, Y., Seo, Y., 2008. A study on the estimation of fugitive PM10 emission in the metropolitan area. In: Proceeding of the 47th Meeting of KOSAE. Korean Society for Atmospheric Environment, pp. 367–368 (2008).

Jickells, T.D., An, Z.S., Andersen, K.K., Baker, A.R., Bergametti, G., Brooks, N., Cao, J.J., Boyd, P.W., Duce, R.A., Hunter, K.A., Kawahata, H., Kubilay, N., laRoche, J., laRoche, J., Liss, P.S., Mahowald, N., Prospero, J.M., Ridgwell, A.J., Tegen, I., Torres, R., 2005. Global iron connections between desert dust, ocean biogeochemistry, and climate. Science 308, 67–71.

Kiley, C.M., Fuelberg, H.E., Palmer, P.I., Allen, D.J., Carmichael, G.R., Jacob, D.J., Mari, C., Pierce, R.B., Pickering, K.E., Tang, Y., Wild, O., Fairlie, T.D., Logan, J.A., Sachse, G.W., Shaack, T.K., Streets, D.G., 2003. An intercomparison and

evaluation of aircraft-derived and simulated CO from seven chemical transport models during the TRACE-P experiment. Journal of Geophysical Research 108, 8819.
Kurosaki, Y., Mikami, M., 2004. Effect of snow cover on threshold wind velocity of dust outbreak. Geophysical Research Letters 31, L03106.
Kwon, H.-J., Cho, S.-H., Chun, Y., Lagarde, F., Pershagen, G., 2002. Effects of the Asian dust events on daily mortality in Seoul, Korea. Environmental Research 90, 1–5.
Lim, J.-Y., Chun, Y., 2006. The characteristics of Asian dust events in Northeast Asia during the springtime from 1993 to 2004. Global and Planetary Change 52, 231–247.
Liu, H., Jacob, D.J., Bey, I., Yantosca, R.M., 2001. Constraints from 210Pb and 7Be on wet deposition and transport in a global three-dimensional chemical tracer model driven by assimilated meteorological fields. Journal of Geophysical Research 106, 12109–12128.
Liu, M., Westphal, D.L., Wang, S., Shimizu, A., Sugimoto, N., Zhou, J., Chen, Y., 2003. A high-resolution numerical study of the Asian dust storms of April 2001. Journal of Geophysical Research 108, 8653.
Marticorena, B., Bergametti, G., 1995. Modeling the atmospheric dust cycle: 1. Design of a soil-derived dust emission scheme. Journal of Geophysical Research 100, 16415–16430.
Martonchik, J.V., Diner, D.J., Kahn, R., Gaitley, B., Holben, B.N., 2004. Comparison of MISR and AERONET aerosol optical depths over desert sites. Geophysical Research Letters 31, L16102.
Miller, R.L., Tegen, I., Perlwitz, J., 2004. Surface radiative forcing by soil dust aerosols and the hydrologic cycle. Journal of Geophysical Research 109, D04203.
Mueller, K.L., Gourdji, S.M., Michalak, A.M., 2008. Global monthly averaged CO_2 fluxes recovered using a geostatistical inverse modeling approach: 1. Results using atmospheric measurements. Journal of Geophysical Research 113, D21114.
Palmer, P.I., Jacob, D.J., Jones, D.B.A., Heald, C.L., Yantosca, R.M., Logan, J.A., Sachse, G.W., Streets, D.G., 2003. Inverting for emissions of carbon monoxide from Asia using aircraft observations over the western Pacific. Journal of Geophysical Research 108, 8828.
Park, R.J., Jacob, D.J., Field, B.D., Yantosca, R.M., Chin, M., 2004. Natural and transboundary pollution influences on sulfate-nitrate-ammonium aerosols in the United States: implications for policy. Journal of Geophysical Research 109, D15204.
Park, R.J., Jacob, D.J., Kumar, N., Yantosca, R.M., 2006. Regional visibility statistics in the United States: natural and transboundary pollution influences, and implications for the Regional Haze Rule. Atmospheric Environment 40, 5405–5423.
Park, S.-U., In, H.-J., 2003. Parameterization of dust emission for the simulation of the yellow sand (Asian dust) event observed in March 2002 in Korea. Journal of Geophysical Research 108, 4618.
Prospero, J.M., 1999. Long-term measurements of the transport of African mineral dust to the southeastern United States: implications for regional air quality. Journal of Geophysical Research 104, 15917–15927.
Prospero, J.M., Ginoux, P., Torres, O., Nicholson, S.E., Gill, T.E., 2002. Environmental characterization of global sources of atmospheric soil dust identified with the NIMBUS 7 Total Ozone Mapping Spectrometer (TOMS) absorbing aerosol product. Reviews of Geophysics 40, 1002.
Rodgers, C.D., 2000. Inverse Methods for Atmospheric Sounding: Theory and Practice. World Sci.
Seinfeld, J.H., Carmichael, G.R., Arimoto, R., Conant, W.C., Brechtel, F.J., Bates, T.S., Cahill, T.A., Clarke, A.D., Doherty, S.J., Flatau, P.J., Huebert, B.J., Kim, J., Markowicz, K.M., Quinn, P.K., Russell, L.M., Russell, P.B., Shimizu, A., Shinozuka, Y., Song, C.H., Tang, Y., Uno, I., Vogelmann, A.M., Weber, R.J., Woo, J.-H., Zhang, X.Y., 2004. ACE-ASIA: regional climatic and atmospheric chemical effects of Asian dust and pollution. Bulletin of the American Meteorological Society 85, 367–380.
Seinfeld, J.H., Pandis, S.N., 1998. Atmospheric Chemistry and Physics. Wiley, New York, p. 1326.
Sokolik, I.N., Toon, O.B., 1996. Direct radiative forcing by anthropogenic airborne mineral aerosols. Nature 381, 681–683.
Tanaka, T.Y., Chiba, M., 2006. A numerical study of the contributions of dust source regions to the global dust budget. Global and Planetary Change 52, 88–104.
Tegen, I., Fung, I., 1994. Modeling of mineral dust in the atmosphere: sources, transport, and optical thickness. Journal of Geophysical Research 99, 22897–22914.
Torres, O., Bhartia, P.K., Herman, J.R., Ahmad, Z., Gleason, J., 1998. Derivation of aerosol properties from satellite measurements of backscattered ultraviolet radiation: theoretical basis. Journal of Geophysical Research 103, 17099–17110.
Uno, I., Carmichael, G.R., Streets, D.G., Tang, Y., Yienger, J.J., Satake, S., Wang, Z., Woo, J.-H., Guttikunda, S., Uematsu, M., Matsumoto, K., Tanimoto, H., Yoshioka, K., Iida, T., 2003. Regional chemical weather forecasting system CFORS: model descriptions and analysis of surface observations at Japanese island stations during the ACE-Asia experiment. Journal of Geophysical Research 108, 8668.
Uno, I., Wang, Z., Chiba, M., Chun, Y.S., Gong, S.L., Hara, Y., Jung, E., Lee, S.S., Liu, M., Mikami, M., Music, S., Nickovic, S., Satake, S., Shao, Y., Song, Z., Sugimoto, N., Tanaka, T., Westphal, D.L., 2006. Dust model intercomparison (DMIP) study over Asia: overview. Journal of Geophysical Research 111, D12213.
Werner, M., Tegen, I., Harrison, S.P., Kohfeld, K.E., Prentice, I.C., Balkanski, Y., Rodhe, H., Roelandt, C., 2002. Seasonal and interannual variability of the mineral dust cycle under present and glacial climate conditions. Journal of Geophysical Research 107, 4744.
White, B.R., 1979. Soil transport by winds on Mars. Journal of Geophysical Research 84, 4643–4651.
Wiscombe, W.J., 1980. Improved Mie scattering algorithms. Applied Optics 19, 1505–1509.
Yoshida, Y., Wang, Y.H., Shim, C., Cunnold, D., Blake, D.R., Dutton, G.S., 2006. Inverse modeling of the global methyl chloride sources. Journal of Geophysical Research 111, D16307.
Yumimoto, K., Uno, I., Sugimoto, N., Shimizu, A., Liu, Z., Winker, D.M., 2008. Adjoint inversion modeling of Asian dust emission using lidar observations. Atmospheric Chemistry and Physics 8, 2869–2884.
Yumimoto, K., Uno, I., Sugimoto, N., Shimizu, A., Satake, S., 2007. Adjoint inverse modeling of dust emission and transport over East Asia. Geophysical Research Letters 34, L08806.
Zender, C.S., Bian, H., Newman, D., 2003a. Mineral dust entrainment and deposition (DEAD) model: description and 1990s dust climatology. Journal of Geophysical Research 108, 4416.
Zender, C.S., Newman, D., Torres, O., 2003b. Spatial heterogeneity in aeolian erodibility: uniform, topographic, geomorphic, and hydrologic hypotheses. Journal of Geophysical Research 108, 4543.
Zhang, L., Gong, S., Padro, J., Barrie, L., 2001. A size-segregated particle dry deposition scheme for an atmospheric aerosol module. Atmospheric Environment 35, 549–560.
Zhang, X.Y., Gong, S.L., Shen, Z.X., Mei, F.M., Xi, X.X., Liu, L.C., Zhou, Z.J., Wang, D., Wang, Y.Q., Cheng, Y., 2003a. Characterization of soil dust aerosol in China and its transport and distribution during 2001 ACE-Asia: 1. Network observations. Journal of Geophysical Research 108, 4261.
Zhang, X.Y., Gong, S.L., Zhao, T.L., Arimoto, R., Wang, Y.Q., Zhou, Z.J., 2003b. Sources of Asian dust and role of climate change versus desertification in Asian dust emission. Geophysical Research Letters 30, 2272.
Zhao, T.L., Gong, S.L., Zhang, X.Y., Jaffe, D.A., 2008. Asian dust storm influence on North American ambient PM levels: observational evidence and controlling factors. Atmospheric Chemistry and Physics 8, 2717–2728.